

Age-related changes in the physical properties, cross-linking, and glycation of collagen from mouse tail tendon

Melanie Stammers¹, Irina M. Ivanova^{1,2}, Izabella S. Niewczas¹, Anne Segonds-Pichon¹, Matthew Streeter³, David A. Spiegel³, Jonathan Clark^{1*}

1) Babraham Institute, Cambridge, CB22 3AT, United Kingdom.

2) John Innes Centre, Norwich Research Park, Norwich, NR4 7UH, United Kingdom.

3) Department of Chemistry, Yale University, 225 Prospect Street, New Haven, CT06511, USA

Running title: *Changes in collagen crosslinks and glycation with age*

*corresponding author jonathan.clark@babraham.ac.uk

Keywords: Tendon, collagen, crosslinks, lysine glycation, aging, physical strain, chemistry, diabetes, mechanical stress, connective tissue

Abstract

Collagen is a structural protein whose internal cross-linking critically determines the properties and functions of connective tissue. Knowing how the cross-linking of collagen changes with age is key to understanding why the mechanical properties of tissues change over a lifetime. The current scientific consensus is that collagen cross-linking increases with age and that this increase leads to tendon stiffening. Here, we show that this view should be reconsidered. Using MS-based analyses, we demonstrate that during aging of healthy C57BL/6 mice, the overall levels of collagen cross-linking in tail tendon decrease with age. However, the levels of lysine glycation in collagen, which is not considered a cross-link, increased dramatically with age. We found that in 16-week-old diabetic db/db mice, glycation reaches levels similar to those observed in 98-week-old C57BL/6 mice, while the other cross-links typical of tendon collagen either decreased or remained the same as those observed in 20 week old WT mice. These results, combined with findings from mechanical testing of tendons from these mice, indicate that overall collagen cross-linking in mouse tendon decreases with age. Our findings also reveal that lysine glycation appears to be an

important factor that contributes to tendon stiffening with age and in diabetes.

Main

The literature surrounding the mechanical and chemical properties of collagen and changes which occur with age is extensive. The general consensus is that as collagen ages there is an increase in the stiffness with loss of elasticity, and that this is due to an increase in covalent intermolecular crosslinking between collagen molecules which develops with age¹. In this paper we challenge the simplicity of this conclusion.

The collagen crosslinking can be divided into two groups, those that are of enzymatic origin and those which form through purely chemical reactions with reactive molecules perfusing the tissues. The enzymatically derived crosslinks that are first formed can be analysed after reduction with sodium borohydride^{2,3} and the reduced products measured as dihydroxy-lysino-norleucine (DHLNL), hydroxy-lysino-norleucine (HLNL) and lysino-norleucine (LNL) (structures shown in figure 1). Another collagen crosslink, HHMD (histidine-hydroxy merodesmosine) is commonly found during the analysis of reduced samples⁴ by mass spectroscopy. While there has been

disagreement^{5,6} with respect to the exact chemical structure the analysed compound represents within collagen, for the purposes of this publication it can be considered an indicator of aldol crosslinks present in collagen before analysis.

These crosslinks are early structures in the enzymatic crosslinking process and are often described as immature crosslinks. The immature crosslinks can go on to form irreversible crosslinks¹ (pyridinolines) often described in the literature as "mature" crosslinks through further reactions. It has been noted in numerous papers that the number of immature crosslinks per mole of collagen decreases with age and that the increase in mature pyridinoline crosslinks does not seem to match this decrease^{7,8,9}, implying that the loss of immature crosslinks cannot be entirely explained by their conversion into mature crosslinks. In papers describing mature crosslink formation the emphasis is usually on the increase in mature crosslinks and correlating this increase to an increase in stiffness of the tissue, however, this overlooks the fact that there is potentially an overall decrease in crosslinking with age from the loss of the immature crosslinks. The paradox here is that if total crosslinking is decreasing with age, then how is it that the tissues get stiffer?

Crosslinks formed through non-enzymatic processes involving sugars are referred to as Advanced Glycation Endproducts (AGEs) and in this text we include them when referring to mature crosslinks. These are formed through the reaction of sugars or products of sugar metabolism with collagen which then react further to create crosslinks. The AGE crosslinks generally considered to be most important are glucosepane and pentosidine^{9,10}. A significant proportion of the literature has focused on increased AGE crosslinking, particularly glucosepane, as a potential cause of stiffening in ageing tendon. This has been concluded through correlations of measured AGE crosslink levels with the mechanical testing of diabetic tissue and of collagen incubated in-vitro in the presence of sugars. However, these studies do not measure the absolute glucosepane concentration as a proportion of the total

collagen content, but usually as a relative increase in signal¹¹ or as a proportion of the extracted insoluble collagen content¹². Here we measure the absolute glucosepane content as a proportion of the total collagen content of tendon in addition to the pentosidine content and the glycation products of lysine and hydroxylysine. Although increases in glucosepane with age have been demonstrated, without knowing the absolute amount relative to the total collagen content it is impossible to assess if glucosepane crosslinking is an important factor in the stiffening of normal healthy tendon during ageing and what the impact of other AGEs might be.

In this study we chose to use mouse tail tendon because it is primarily collagen I and the impact of altered crosslinking on the mechanical properties can be readily tested. We used tendon from wild type C57BL/6 mice because they have been shown not to develop diabetes¹³ and so represent a model of healthy ageing. We studied both the mechanical and chemical changes across a population of mice from 8 weeks to 100 weeks old. In order to remove as many population variables as possible and show what happens in the normal, healthy ageing process, a cohort of C57BL/6 mice housed under highly controlled conditions of diet and environment were used.

The aim of the study described here is to clarify the quantitative changes in crosslinking that occur in normal healthy mouse tail tendon with age and identify which crosslinks are likely to give rise to the altered physical properties with age.

Results

Confirmation of basic mouse model parameters. Blood glucose levels were found to be controlled well across all age groups under fasting and non-fasting conditions (Figure S1a,b).

The approximate rate of collagen synthesis in tendon at 33, 63 and 88 weeks of age was determined by feeding ¹³C₆ Lysine for 28 days and then measuring the incorporation of the label into the collagen within the tissues. The rate of incorporation of ¹³C₆ Lysine was found to

be between 0.04% and 0.06% collagen lysine content per day in tail tendon showing little change with age. (Figure S1c).

Profiling changes in the physical properties of tail tendon with age.

The stress-strain profiles for multiple tail tendons from 5 mice from a range of ages were measured using a tensile stress stage. There are 4 tendons for each vertebral bone in the tail which run from the base of the tail to each bone insertion point in four bundles of tendons. The individual tendons were carefully dissected out from the bundles for use. Individual tendons were stretched to breaking point at a rate of 1mm/min and the stress measured every 0.5s. The stress-strain profiles (Figure 2) for the fibres from younger animals were more homogeneous across the population than those from older animals. Tendon from 10 week old mice showed an initial stretching phase followed by a long plastic extension phase before breaking. The stress-strain profile of tendons from older animals had a much greater spread, some fibres still showing a plastic extension phase, with others breaking earlier at a lower strain with only a modest plastic extension phase. With increasing age a greater proportion of the tendons showed an increase in the gradient of the initial stretching phase, that is the stiffness (Young's Modulus) of the tendons increases. The initial stretching phase in animals of all ages extended to about 5% strain before transitioning into the plastic phase. Young adult tendons in the 20 week group frequently reached a greater strain before breaking than that seen in either younger tendons or tendons greater than 1 year. The picture of changes seen here is more subtle than the impression usually presented in the literature where a simplified schematic of increasing stiffness of tendon with age is shown.

Crosslink profiles with age. The crosslinks present and collagen content were measured by HPLC mass spectroscopy using tissue processing and mass spectroscopy methods developed for this project. Of particular concern to us was to remove reactive soluble compounds released from cell lysis, such as ribose-5-phosphate which are known to be highly reactive glycosylating molecules. To do this we used a

continuous flow system to wash the soluble components from the samples. We confirmed that the processing method for removal of soluble components did not impact the proportions of analytes under study by comparing the levels in tendon immediately after dissection without processing and after processing. In addition to this, a novel method for the analysis of the AGE crosslink glucosepane by mass spectroscopy was developed where the acid hydrolysis products of both the endogenous and synthetic $^{13}\text{C}_5$ labelled glucosepane spiked into the sample before hydrolysis were measured.

Figure 3 shows changes in the crosslinks found in mouse tail tendon with age. The most abundant crosslink at all ages was HLNL and the greatest change with age occurred in the level of this crosslink. A large drop in HLNL occurred up to 20 weeks when the animal was maturing, decreasing from 3 crosslinks per collagen molecule at 8 weeks to 1.5 crosslinks per collagen molecule at 20 weeks. HLNL levels continued to decrease more gradually after the animal had matured, falling to approximately 0.85 crosslinks per collagen molecule at 96 weeks.

While we could not quantify the absolute amount of HHMD due to the lack of a synthetic standard, we were able to measure the relative change in the mass spectrometer detector response. HHMD can be seen to increase significantly up to 20-36 weeks and then significantly decrease as the animals age (Figure 3d). Both HHMD and HLNL are formed from aldehydes generated by the activity of lysyl oxidase. The aldehydes could also be produced from the hydrolysis of HLNL, and because we saw a large drop in HLNL up to 20 weeks we looked at whether a correlation between HLNL and HHMD could be seen. There were clearly two phases in the data shown in the correlation plots between HLNL and HHMD (Figure 3e). In the first phase between 8 and 36 weeks it can be seen that as HLNL decreases, HHMD increases. In the second phase from 36 to 96 weeks it can be seen that both the HLNL and HHMD decline with age. This data suggests that as the HLNL levels drop rapidly in early life, that the

aldehyde generated undergoes an aldol reaction and HHMD formation faster than any alternative aldehyde or aldol removal process. In later life, the rate of formation of aldol adducts is then slower than the rate of removal and so both the level of HLNL and HHMD measured are seen to decline.

In an attempt to estimate the possible level of HHMD we made an assumption that the HLNL change between the ages of 11 weeks and 20 weeks is converted into the measured change in HHMD based on the correlation seen. With this assumption, the level of HHMD converts to about 1.1 HHMD per collagen molecule at 20 weeks and 0.6 to 0.8 HHMD per collagen molecule at 96 weeks (the conversion factor is approximately 10 HHMD area ratio units to 1 HHMD molecule in Figure 3d). This level of HHMD is broadly consistent with reported levels of the compound found in tendon using tritium labelling and ion-exchange chromatography¹⁴.

No single mature crosslink type increased dramatically with age, however, as a group, mature crosslinks contributed to a modest increase in overall number of crosslinks per collagen molecule (Figure 3l). The increase in mature crosslinks equated to an increase from 1 crosslink per 33 collagen molecules at 10 weeks to 1 crosslink in 5 collagen molecules at 96 weeks. This increase in mature crosslinks was 3 times less than the drop in HLNL between 20 weeks and 96 weeks (see figures 3c and l). The sum of mature and immature crosslinks at 96 weeks was approximately 1 crosslink per collagen molecule excluding the HHMD contribution.

Changes in glycation with age. Over the lifetime of the animals there was only a modest increase in AGE crosslinks, however, in contrast with this the increase in lysine glycation was a major change observed (Figure 3f). The glycation of lysine is the direct addition of a monosaccharide, typically glucose, to the side chain nitrogen of lysine and is not a crosslink. Crosslink formation would require further reaction with another residue in the collagen structure. The addition reaction can also happen on the side chain of hydroxylysine.

By 60 weeks of age the glycation of tendon collagen lysine reached 1.5 per collagen molecule, the glycation of hydroxylysine being much lower at about 0.2 per molecule of collagen. The level of lysine glycation appears to plateau after 50 weeks of age. Increased levels of glycation appear to correlate with decreased HLNL levels, although both were changing rapidly during the growth phase so may not be causally linked (Figure 3i). It has been reported that glycation occurs at the same site as the lysyl oxidase mediated crosslinks¹⁵, however, in that report only glycation of Hly was seen. In our study we see glycation of Lys rather than Hly as the major adduct.

Diabetic tendon. With the changes seen in collagen lysine side chain glycation in healthy wild type C57BL/6 mice, we decided to examine the levels seen in diabetic mice. Tail tendon samples from 16 week old JAX™ db/db mice (Charles River) on C57BLKS/J background were obtained. These diabetic mice have a point mutation in the Lepr gene and are used as an animal model for diabetes research. The tendon fibres were subjected to physical and chemical analysis as described above and the results are shown in Figure 4a & S2. The spread and stiffness observed in the break test profiles of tendon from 16 week db/db mice resembled those seen from older WT animals, while the plastic extension phase often looked more like that from younger animals (less than 1 year). Kinks and wobbles in the profiles of the db/db tendon can be seen in the traces, which were more prevalent than for WT tendon.

Chemical analysis showed that all forms of detectable crosslink for the diabetic animals, apart from HHMD, were lower than the levels found in both 20 week and 96 week WT animals (Figure 4b,c). The HHMD level was not significantly different between 20 week WT and 16 week db/db tendon. The HLNL level in 16 week db/db tendon was found to be approximately 0.6 HLNL bonds per collagen molecule which is much lower than the 1.5 HLNL bonds per collagen molecule found in 20 week WT tendon. The level of glycation in the 16 week db/db tendon was comparable to that from 96 week old WT mice, much higher than

that seen in the 20 week WT mice. The level of irreversible crosslinks in the db/db mice, both the mature and AGE classes, were lower than those seen for 20 week WT mice.

Discussion

Within the literature of ageing collagen the focus is usually on the increase of mature crosslinks formed through mature covalent bonding as the reason for the changing properties observed. What we have seen here shows that the situation is more complex than this and that both the loss of reversible crosslinks and increase in lysine glycation are important changes to consider in the overall picture of how tendon collagen functions.

The often stated view that tendon stiffens with age due to an increase in crosslinking does not fit the entire data set shown here, and in the light of the db/db data it would appear that the mechanical changes do not have to be linked to an increase in AGEs such as glucosepane or pentosidine. With the marked decrease in crosslinking in db/db mice it might be expected that the tendons would be less stiff than older WT mice, however, the stiffness of the db/db tendons is similar to that of older WT mice. The one clear factor that could give rise to the observed stiffness of db/db tendon is the increased glycation of lysine residues which is similar to that found in tendon from 98 week mice. It is apparent from the kinks and wobbles in the db/db stress-strain profiles that there are faults in the tendon structure. It is likely that these faults are due to the lower levels of crosslinking explaining why the diabetic tendon is often unable to maintain structure under stress.

While tendon does generally stiffen with age, another important change is the loss of the plastic extension phase. It seems likely from the results presented here that the loss of the plastic phase is due to a decrease in immature crosslinks with an increase in mature crosslinking, while the stiffening is caused by both the glycation of lysine and mature crosslink formation. The mechanisms by which crosslinks contribute to these properties and a demonstration of the involvement of glycated

lysine in tendon functioning is the subject of a parallel manuscript²².

In conclusion, tendon stiffening and the loss of the plastic phase in extension are important mechanical changes with age and diabetes observed in this study. Defining the parameters for healthy ageing requires an understanding of the underlying chemical changes that underpin these mechanical changes. Here we have identified that lysine glycation products are likely to play a significant role in these mechanical changes as well as the altered distribution of immature and mature enzymatic crosslinks.

Experimental

Animal procedures:

Ethics. Animal experiments were performed according to the UK Animals (Scientific Procedures) Act 1986, licence PPL 70/8303 and approved by the Babraham Institute Animal Welfare and Ethics Review Body.

Blood glucose measurements. Cohorts of C57Bl/6 mice were culled using the standard schedule 1 method of CO₂ exposure for killing the mice followed by cardiac bleed as the secondary method of confirmation. The glucose level was measured in the blood from the cardiac bleed and from a drop of blood taken from the tail vein after culling. The blood glucose level was measured using SD CodeFree blood glucose strips from SD Biosensor.

Labelling with ¹³C₆ Lysine. Cohorts of C57Bl/6 mice were fed on MouseExpress (¹³C₆, 99%) L-Lysine irradiated mouse feed from CK Isotopes for 28 days. After day 28 the mice were switched to a normal diet for a further 7 days and then culled.

Sample analysis:

Tissue processing. After removal of the skin from isolated tails, tendon was drawn out of the tail under PBS pH 7.4 by grasping the tip and the base of the tail with forceps. Twisting the forceps holding the tip caused the tail to break bringing attached tendon fibres with it attached

to the vertebral bone. Tendon was isolated sequentially one vertebral bone at a time, working up the tail from the tip to the base. Tendon fibres were detached from the tail vertebrae with a scalpel. Cellular and soluble extracellular components were removed from tail tendon by washing in 3% triton in a continuous flow system (~200ml / 24 hours) for 3 days, followed by washing in water for 2-3 days (~200ml / 24 hours).

Of note here is that the chemistry of the immature crosslinks is potentially reversible, any processing that changes chemical environment before reduction could perturb the equilibrium and impact the results^{16,17}. For example, when we incubated skin with a 50% glycerol solution in PBS pH 7.4 for 2 hours we found after reduction there was a 37% drop in the level of HLNL and a 27% drop in Lys glycation. Figure S3 shows the impact on tendon collagen of using TES/Tris buffer as commonly used¹⁴ when compared to PBS that we use in this work. It can be seen that in TES/Tris buffer, HLNL is 13% lower and the glycated lysine is 61% lower than that obtained in PBS. Both TES and Tris contain functionality similar to glycerol and could be acting chemically in a similar way.

Acid hydrolysis. Tail tendon (wet weight 16 to 22mg) suspended in 200ul PBS pH7.4 was reduced by the addition of 10ul of 10mg/ml NaBH₄ in 1mM NaOH. After incubation for 2h at room temperature the tendon was washed 3 times with water and then freeze dried. Lipid was removed by the addition of 1ml CHCl₃/MeOH/H₂O (100:50:5). After incubation overnight at room temperature the tendon was washed with a further 1ml CHCl₃/MeOH/H₂O (100:50:5) before air drying and freeze drying. ¹³C₅ Glucosepane internal standard was added and samples freeze dried. Acid hydrolysis was carried out by incubation overnight at 95°C with 200ul of 7.4M HCl. Samples were then dried under a stream of nitrogen gas and resuspended in 400ul 30% MeCN / 0.1% formic acid. After filtering through a 0.22um nylon filtration membrane samples were freeze dried before resuspension at 10ug/ul (dry weight) in 30% MeCN / 0.1% formic acid. Solutions were then made up at different concentrations with

appropriate internal standards for the analysis of the different analytes.

HPLC-MS method. 5ul of solution for analysis was injected onto a Cogent Diamond Hydride column (4um, 100A, 150 x 2.1mm). Diamond Hydride columns have been described in the analysis of amino acids¹⁸ and collagen crosslinks¹⁹. The method here is a modification of these protocols. A gradient of 100% (Acetonitrile, 5% water, 0.1% formic acid, 0.005% trifluoroacetic acid) to 100% (Water, 0.1% formic acid) was run, the details of which are in table 1 below. The flow was passed into an esi probe of a Micromass Quattro Ultima mass spectrometer and the fragmentation transitions listed below, monitored. (Mass Spectrometer parameters: source temperature 120°C, desolvation temperature 350°C, cone voltage 3kV, capillary voltage 35V, collision gas was argon, collision voltage - see table 2).

Glycated lysine and glycated hydroxylysine are known to undergo partial cyclisation under the acid hydrolysis conditions. Both the linear (Hx) and cyclic (cHx) forms were measured and the result added to give the total glycated lysine and total glycated hydroxylysine values.

Calibrations. Amino acid calibration curves were made using commercially available amino acid mix from Sigma Aldrich (A9906 lot SLBR9938V). Calibration curves were constructed using 2,3,3,4,4,5,5-d7- DL-Pro (CK Isotopes) as internal standard for Pro, Hyp and 4,4,5,5-d4-L-Lysine as internal standard for Lys and Hly.

HLNL, LNL and DHLNL (Santa Cruz Biotechnology Inc.) were used for calibration curves with d4-lysine (Sigma Aldrich) as an internal standard. The standards and ISD were spiked into acid hydrolysed collagen (50ug) which had not been reduced for the calibration curve.

DPD (Polypeptide Group) was used to construct a calibration curve against d4 Lysine as the internal standard. Calibration curves were constructed separately and confirmed for DPD and PYD with a PYD/ DPD HPLC mixture (Quidel Corporation).

$^{13}\text{C}_6$ Hx-Lysine, $^{12}\text{C}_6$ Hx-Lysine and $^{12}\text{C}_6$ cHx-lysine were made in house as standards to enable calibration curves to be constructed. The response of the $^{13}\text{C}_6$ Hx-Lysine ISD was found to be the same as that for $^{12}\text{C}_6$ Hx-Lysine. The response of $^{12}\text{C}_6$ cHx-lysine was found to be a factor of 1.149 less than that for the $^{13}\text{C}_6$ Hx-Lysine ISD.

d4-L-Lysine was used as internal standard for HHMD at 50ug sample injections and ^{13}C -Hx-Lys used for 400ug sample injections.

Glucosepane analysis. $^{13}\text{C}_5$ Glucosepane made from $^{13}\text{C}_5$ ornithine was kindly provided by David Spiegel (Yale), synthesised according to his published methods²⁰ along with synthetic ^{12}C Glucosepane. The usual method for measuring glucosepane is to use extensive proteolytic digests of collagen with a series of enzymes over two weeks rather than acid hydrolysis because glucosepane is not considered to be stable to acid. There are a number of issues with the proteolytic digest method, one is the time it takes to carry out the digests which does not lend itself to large numbers of samples, and another is that we found, as others have¹¹, that you are left with a precipitate which is spun down and discarded. Conceptually the discarding of a precipitate seems to be at odds with the complete measurement of crosslinks because it is possible that this precipitate might contain the very crosslinks that you are interested in. We found that when glucosepane is hydrolysed in acid, that there is an addition of one molecule of water to the structure by mass spectroscopy. By the inclusion of a ^{13}C labelled glucosepane standard before hydrolysis, we found that glucosepane could be measured reliably after hydrolysis by measurement of this adduct. Experiments were carried out to test the method by spiking in both ^{13}C and ^{12}C glucosepane at different concentrations into collagen samples prior to hydrolysis. We have not explored how universally applicable this method is for the analysis of glucosepane in tissues other than mouse skin and mouse tendon.

HHMD identification and analysis. Parent scans on the mass spectrometer were carried out looking for molecular ions in reduced tendon samples that gave rise to a fragment m/z of 82, a

typical fragmentation product of hydroxylysine residues. An expected ion of 574.3 was found at 9.4 minutes which was in the expected retention time range on the HPLC system for a structure of the type proposed by Tanzer⁴. Fragmentation of the 574.3 ion gave a fragmentation pattern (Figure S4) consistent with the proposed structure.

We then carried out a comparison of the Lys m/z 84 fragment and Hly m/z 82 fragments after NaBH_4 reduction, and the Lys m/z 85 and Hly m/z 83 fragments after NaBD_4 reduction. This experiment was to identify the position of the putative imine bond in the un-reduced structure. The results from this experiment are shown in (Figure S5). This data when extrapolated to the precursor before reduction, shows that in the un-reduced sample there is Hly, a proportionately small amount of imine from Hly aldehyde, a Lys fragment and a similar level of imine from Lys-aldehyde to the level of the Lys fragment. The proportions of Hly, Lys and deuterated Lys fragments is consistent with the structure shown in Tanzer's paper. Fragmentation of the m/z ion 575 from NaBD_4 reduction (Figure S6) clearly showed reduction occurring on the "core" and no core fragments without deuterium which is consistent with the structure proposed by Tanzer.

The conclusion that we came to was that the m/z 574 ion seen here is consistent with the proposed structure and we proceeded on the basis that it was likely to be the same compound that Tanzer analysed and called HHMD.

Chemical synthesis:

All non-labelled reagents used were obtained from Sigma Aldrich and stable isotopically labelled compounds from CK Isotopes Ltd (UK). Solvents were obtained from Romil Ltd (Cambridge, UK) and were either super pure or ultra pure grades. Mass spectra were run on Sciex QTRAP4000 and Micromass Quattro Ultima mass spectrometers. NMR spectra were run on a Bruker 500MHz DCH Cryoprobe spectrometer in the University of Cambridge Chemistry Department.

***N*-deoxyhexitoyl-L-lysine (Lys-Hx) synthesis.** The following synthesis produced an inseparable

mixture of ϵ N-glycated lysine (by NMR) which looked the same as endogenous glycated lysine by mass spectroscopy. It is likely that some racemisation occurred at chiral centres in this synthesis and this accounts for some or all of the additional complexity seen in the NMR spectra. This synthesis enabled a $^{13}\text{C}_6$ internal standard to be synthesised which behaved well in the mass spectroscopy assay.

N α -benzyloxycarbonyl-L-lysine (200mg, 1eq) was added to glucose (1.55g, 12eq) in methanol (30ml). The reaction was refluxed for 4 hours and then allowed to cool. Sodium borohydride (324mg, 12eq) was then added and the reaction left to stir overnight. 1M Hydrochloric acid (3ml) was then added and the solution concentrated to an oil. Water (30ml) was added and the pH adjusted to 4. The solution was loaded onto a 5g C18 SPE cartridge (BondElute, Varian), washed with 5mM HCl (20ml) and the glycated materials eluted with 10% acetonitrile. The solution was then freeze dried. HPLC showed a number of peaks which were analysed by mass spectroscopy. The largest peak had the correct mass of 445.5 (MH⁺). Starting with the crude glycated material (80 mg), pure mono glycated Z-Lys (14mg) was isolated after 3 rounds of purification on a C18 Luna 10x250mm column with a 5% to 50% B gradient (A: (water 0.1% TFA) B: (acetonitrile 90%, water 10%, 0.1% TFA)).

The deoxyhexitolyl- N α -benzyloxycarbonyl-L-lysine (10mg) was then added to water (1ml) with methanol (0.2ml) and 10% Pd/C (3.8mg). The reaction was placed under hydrogen at atmospheric pressure and left for 1.5 hours. Completion of reaction was checked by mass spectroscopy. The Pd/C was removed by filtering the reaction through a 3000 molecular weight cut off filter and freeze dried to give 4mg of the desired product 6-(2,3,4,5,6-pentahydroxyhexylamino)-2-aminohexanoic acid (**Lys-Hx**).

The retention time and fragmentation pattern matched that of endogenous glycation with a parent m/z of 311.18. NMR data shown in S7a-f (1H, 13C, DEPT135, 1H COSY, HSQC, HMBC). Fragmentation pattern shown in S8.

This synthesis was repeated for both $^{12}\text{C}_6$ and $^{13}\text{C}_6$ glucose. For the $^{13}\text{C}_6$ glucose reaction the quantity of the reagents were scaled down and a ratio of 1:1 $^{13}\text{C}_6$ glucose : Z-Lys was used.

2-amino-6-(3,4,5-trihydroxy-2-(hydroxymethyl)piperidin-1-yl)hexanoic acid (Lys-cHx) synthesis. 2,3,4,6-Tetrabenzyl glucose (1g, 1eq) was suspended in methanol (50ml) and water (70ml). 1,4 Dioxane (40ml) was added and solution was warmed up gently to 40°C. Sodium borohydride (210mg, 3eq) was added in 1mM sodium hydroxide solution (1ml). The reaction was stirred overnight but was found to be only 50% complete by TLC (toluene : ethyl acetate 4:1). Additional portion of sodium borohydride (210mg, 3eq) was added and stirred until complete (24 hours). 1M hydrochloric acid (3ml) in water (10ml) followed by EtOAc (60ml) was added to the reaction, the organic layer separated, dried over MgSO₄ and concentrated under vacuum. The product was purified on silica with toluene : ethyl acetate 7:3 as eluent to provide pure product 2,3,4,6-tetrakis(benzyloxy)hexane-1,5-diol (745mg, 75% yield). NMR spectra are in agreement with previously reported data²¹. ESI mass spectroscopy gave m/z 543.27, MH⁺.

DMSO (105ul, 8eq) was added to CH₂Cl₂ (4ml) and cooled down to -78°C. A solution of trifluoroacetic anhydride (153ul, 6eq) in CH₂Cl₂ (1ml) was added dropwise over 20 minutes and left to react for further 10 minutes. 1,3,4,5-tetrabenzyl (2S,3R,4R,5R)-Hexane-1,2,3,4,5,6-hexol (100mg, 1eq) in CH₂Cl₂ (1ml) was added dropwise over 15 minutes. The reaction was stirred for 45 minutes and then triethylamine (257ul, 10eq) added over 10 minutes and left to react for additional 10 minutes. The reaction mixture was allowed to warm up to room temperature over 30 minutes and left to stir for a further 1 hour. Saturated brine was added and the product extracted into CH₂Cl₂, dried over MgSO₄ and concentrated. The crude dicarbonyl product was taken onto the next step without purification.

NaBH₃CN (46.8mg, 4eq) and Na₂SO₃ (93mg, 4eq) were added to the stirred solution of N α -benzyloxycarbonyl-L-lysine benzyl ester (82.5mg, 1.18eq) in methanol (0.5 ml). The

reaction was cooled down in the ice bath and stirred for 10 min, then the dicarbonyl product (prepared above) was added as methanol solution (1.5ml). After 20 min the reaction mixture was warmed up to room temperature and stirred for 20 hours. The solvent was evaporated, residue dissolved in dichloromethane and washed with 1M sodium bicarbonate solution. The organic phase was dried over MgSO₄ and concentrated under vacuum at room temperature. The crude product was purified on silica with toluene : ethyl acetate 95:5 (with 0.5% Et₃N added) as the eluent followed by crystallization from methanol to afford benzyl-1-((benzyloxy)carbonyl)-5-(3,4,5-trihydroxy-2-(hydroxymethyl)piperidin-1-yl)pentyl carbamate as a white powder (8mg, 5% yield). 1H NMR data shown in S9. ESI mass spectroscopy gave m/z 877.52 MH⁺.

Benzyl-1-((benzyloxy)carbonyl)-5-(3,4,5-trihydroxy-2-(hydroxymethyl)piperidin-1-yl)pentyl carbamate (7mg, 1eq) was dissolved in ethyl acetate (0.5ml) followed by addition of methanol: water (1:1, 2ml). 1M Hydrochloric acid (27ul, 3.4eq) was added followed by 10% Pd/C (20mg). The reaction was stirred under hydrogen at atmospheric pressure and progress was monitored by mass spectroscopy. After 96 hours, the reaction was filtered through a Costar 0.22um spin filter to remove the Pd/C and concentrated under reduced pressure. The product was freeze dried from water to afford 2-amino-6-(3,4,5-trihydroxy-2-(hydroxymethyl)piperidin-1-yl)hexanoic acid (**Lys-cHx**) (2.6mg, 98% yield). NMR data

Definitions

Stress = Force/cross sectional area

Strain = Extension / initial length

Acknowledgements. The SENS Foundation for their support without which this work would not have been carried out. Professor Melinda Duer (Cambridge University, UK) for helpful discussions and encouragement. NMR spectra were kindly run by Duncan Howe and Andrew Mason (Department of Chemistry, UK).

shown in S10a-e (1H, DQF COSY, TOCSY, 13C, HSQC). ESI mass spectroscopy gave m/z 293.2 MH⁺.

Physical testing:

Stress strain profile measurements. Physical testing was undertaken using a Microtest 200N tensile stress stage (Deben UK Ltd) fitted with a 20N loadcell and a petri-dish bath to allow immersion of the sample. With a distance of 14mm between the jaws, individual processed fibres were clamped submerged in PBS pH 7.4 at room temperature, and pre-loaded to a force of 0.01N. The diameter of each fibre was assessed along its length and the smallest dimension used to calculate stress. Force was measured as the fibre was taken to breaking point at a speed of 1mm/min.

Statistical analysis

Where 2 groups were compared, Ratio paired Student t-tests were used. When more than 2 groups were compared, One-way ANOVA followed by Tukey's multiple comparisons tests were applied. Linear and non-linear regressions were applied to quantify the association between continuous variables. Significance was defined as p<0.05 and p-values are reported on figures. Data analysis was performed using GraphPad Prism 8.

Funding

JC, M.Stammers, II funded by SENS Research Foundation. Imaging, Chemistry, Mass Spectroscopy and Statistical Analysis were carried out in Babraham Institute facilities which are part funded by Babraham Institute's Core Capability Grant from the BBSRC.

Author contributions

JC, M.Stammers, II, IN designed and performed experiments and analysed data. AS-P carried out statistical analysis. JC wrote the paper and directed the research. M.Streeter and DAS synthesised and provided the ^{12}C and ^{13}C labelled glucosepane standards.

Competing interests

The authors declare no competing financial interests.

Data availability

All data are available from the corresponding author upon reasonable request.

References

1. Collagen Structure and Mechanics Editor Fratzl, Peter. 2008 ISBN 978-0-387-73906-9
2. Bailey, A. J. & Peach, C. M., Isolation and structural identification of a labile intermolecular crosslink in collagen. *Biochem. Biophys. Res. Commun.* 33, 812-819 (1968)
3. Tanzer, M. L., Mechanic, G. & Gallop, P. M., Isolation of Hydroxylysinoxorleucine and its lactone from Reconstituted Collagen Fibrils. *Biochim. Biophys. Acta* 207, 548-552 (1970).
4. Tanzer, M. L., Housley, T., Berube, L., Fairweather, R., Franzblau, C., & Gallop, P. M. Structure of Two Histidine-containing Cross- Links from Collagen. *The Journal of Biological Chemistry*, 248(2), 393-402 (1973).
5. Bernstein, P. H., Mechanic, G. L. A Natural Histidine-based Imminium Cross-link in Collagen and Its Location. *The Journal of Biological Chemistry*, 255 (21), 10414-10422 (1980).
6. Eyre, D. R., Weis, M. A., & Rai, J. Analyses of lysine aldehyde cross-linking in collagen reveal that the mature cross-link histidinohydroxylysinoxorleucine is an artifact. *Journal of Biological Chemistry*, 294(16), 6578-6590 (2019).
7. Robins, S. P., Shimokomaki, M. & Bailey, A. J., The chemistry of the collagen cross-links. Age-related changes in the reducible components of intact bovine collagen fibres. *Biochem. J.* 131, 771-780 (1973).
8. Sricholpech, M. et al. Lysyl hydroxylase 3-mediated glucosylation in type I collagen: Molecular loci and biological significance. *J. Biol. Chem.* 287, 22998-23009 (2012).

9. Saito, M. & Marumo K., Collagen cross-links as a determinant of bone quality: A possible explanation for bone fragility in aging, osteoporosis, and diabetes mellitus. *Osteoporos. Int.* 21, 195–214 (2010).
10. Monnier, V. M., Sun, W., Sell, D. R., Fan, X., Nemet, I., & Genuth, S., Glucosepane: A poorly understood advanced glycation end product of growing importance for diabetes and its complications. *Clin. Chem. Lab. Med.* 52, 21–32 (2014).
11. Nash, A., Notou, M., Lopez-Clavijo, A. F., Bozec, L., de Leeuw, N. H., Birch, H. L., Glucosepane is associated with changes to structural and physical properties of collagen fibrils. *Matrix Biology Plus*, 4, Article 100013 (2019).
12. Monnier, V. M., Bautista, O., Kenny, D., Sell, D. R., Fogarty, J., Cleary, P. A., Lachin, J., Genuth, S., Collagen Glycation, Glycooxidation, and Crosslinking Are Lower in Subjects With Long-Term Intensive Versus Conventional Therapy of Type 1 Diabetes. *Diabetes* 48(4), 870–880 (1999).
13. Lipson, G. & Harrison, E., Aging and glucose homeostasis in C57BL/6J male mice. *FASEB Journal* 2(12) 2807–2811 (1988)
14. Terajima, M., Taga, Y., Chen, Y., Cabral, W. A., Hou-Fu, G., Srisawasdi, S., Yamauchi, M., Cyclophilin-B modulates collagen cross-linking by differentially affecting lysine hydroxylation in the helical and telopeptidyl domains of tendon type I collagen. *Journal of Biological Chemistry*, 291(18), 9501–9512 (2016).
15. Hudson, D. M., Archer, M., King, K. B., & Eyre, D. R. Glycation of type I collagen selectively targets the same helical domain lysine sites as lysyl oxidase-mediated cross-linking. *Journal of Biological Chemistry*, 293(40), 15620–15627(2018).
16. Davison, P. F., The contribution of labile crosslinks to the tensile behaviour of tendons. *Connect. Tissue Res.* 18, 293–305 (1989).
17. Davison, P. F., Cannon, D.J., Anderson, L. P., The effect of acetic acid on collagen crosslinks. *Connect. Tissue Res.*, 1. 205-216 (1972)
18. Bawazeer, S., Sutcliffe, O. B., Euerby, M. R., Bawazeer, S. & Watson, D. G. A comparison of the chromatographic properties of silica gel and silicon hydride modified silica gels. *J. Chromatogr. A* 1263, 61–67 (2012).
19. Naffa, R., Holmes, G., Ahn, M., Harding, D. & Norris, G. Liquid chromatography-electrospray ionization mass spectrometry for the simultaneous quantitation of collagen and elastin crosslinks. *J. Chromatogr. A* 1478, 60–67 (2016).
20. Draghici, C., Wang, T., Spiegel, D.A., Concise total synthesis of glucosepane. *Science* 350 (6258), 294-298 (2015).
21. Li, Q.R., Kim, S.I., Park, S. J., Yang, H.R. Baek A. R., Kim, I.S., Jung, Y.H., Total synthesis of (+) valienamine and (-)-1-epi-valienamine via a highly diastereoselective allylic amination of cyclic polybenzyl ether using chlorosulfonyl isocyanate. *Tetrahedron* 69, 10384-10390 (2013).
22. Mechanical stretching changes crosslinking and glycation levels in the collagen of mouse tail tendon (parallel paper)

Time / min	% solvent A	% Solvent B	% Solvent C	Flow / ml/min	Curve
0	100	0	0	0.4	1
5	60	40	0	0.4	6
7	10	90	0	0.4	6
9	0	0	100	0.4	1
11	0	0	100	0.4	1
12	100	0	0	0.4	1
20	100	0	0	0.4	1

Table 1 showing HPLC gradient solvent profile. Waters Alliance 2795 HPLC. Solvent A: (95% Acetonitrile, 5% water) 0.1% formic acid, 0.005% Trifluoroacetic acid. Solvent B: (20% Methanol, 80% Water), 0.1% formic acid. Solvent C: Water, 0.1% formic acid. Curve 6 is a linear gradient, Curve 1 is a step change to the indicated percentage solvent.

<u>Molecule</u>	<u>Q1</u>	<u>Q2</u>	<u>Collision energy</u>	<u>dwell /s</u>
Proline (PRO)	116.07	70.06	15	0.25
d7-PRO	123.11	77.11	15	0.25
Hydroxyproline (HYP)	132.06	68.05	20	0.25
Lysine (Lys)	147.11	84.08	20	0.25
d4-LYS	151.14	88.1	20	0.25
Hydroxylysine (Hly)	163.1	82.06	20	0.25
LNL	276.15	84.08	30	0.2
HLNL	292.18	82.08	30	0.2
Cyclic glyated lysine (LYS-cHX)	293.18	84.08	30	0.2
DHLNL	308.18	82.08	35	0.2
Cyclic glyated Hly (HLY-cHX)	309.18	82.08	30	0.2
Glycated (linear) lysine (LYS-HX)	311.18	84.08	30	0.2
13C-Hx_Lys std	317.18	84.08	30	0.2

Glycated (linear) hydroxylysine (Hly-Hx)	327.18	82.08	30	0.2
pentosidine	379.21	187.1	40	0.2
Deoxypyridinoline (DPD)	413.2	84.08	40	0.3
Pyridinoline (PYD)	429.2	82.08	40	0.3
¹³ C Hydrolysed Glucosepane (M+2H ⁺ ion)	226.64	84.08	20	0.2
Hydrolysed Glucosepane (M+2H ⁺ ion)	224.28	84.08	20	0.2
Histidino-hydroxymersodesmine (HHMD)	574.31	156.07	55	0.3
6-Hydroxynorleucine	148.09	102.09	10	0.1
6-D ₁ -6-Hydroxynorleucine	149.13	103.1	10	0.1

Table 2, Mass spectrometer mass transitions table

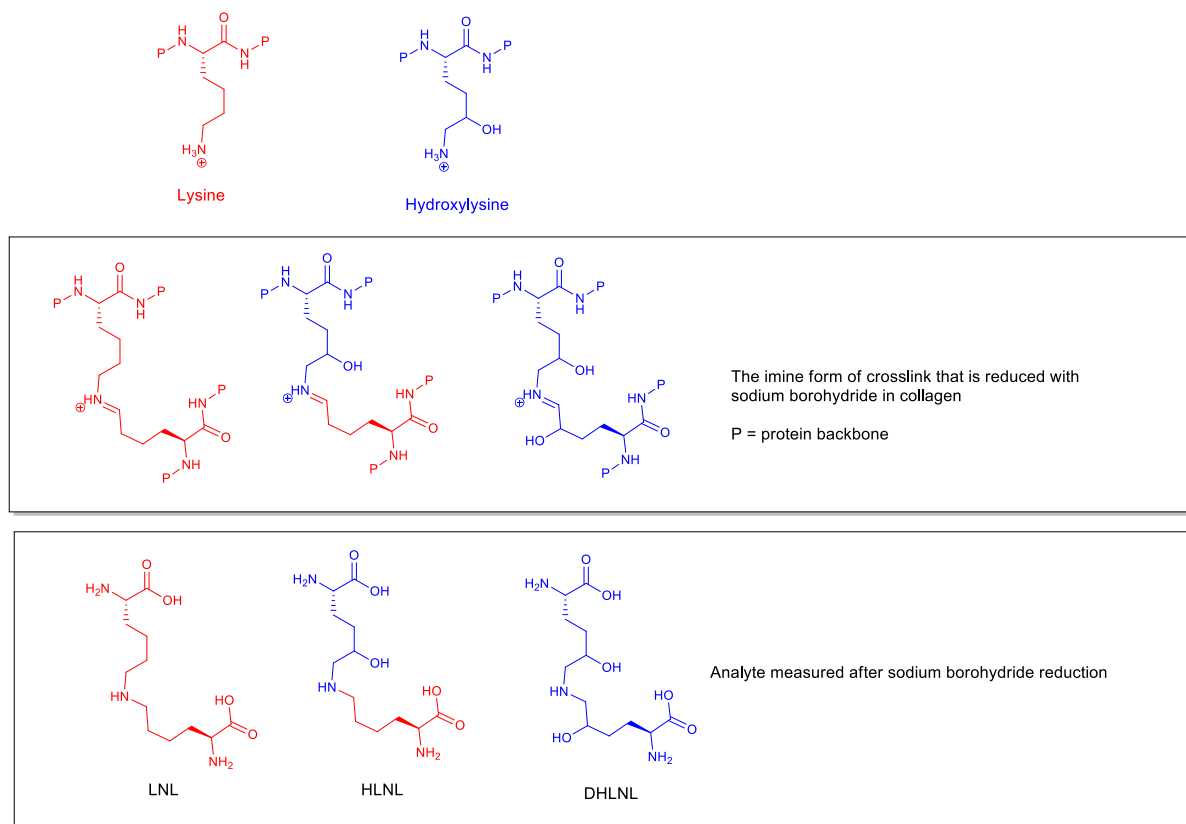


Figure 1 The structures of LNL, HLNL, and DHLNL analysed by mass spectroscopy after treatment with sodium borohydride. The relationship to lysine and hydroxylysine, and the intermediate imine crosslink structures found in collagen are also shown above.

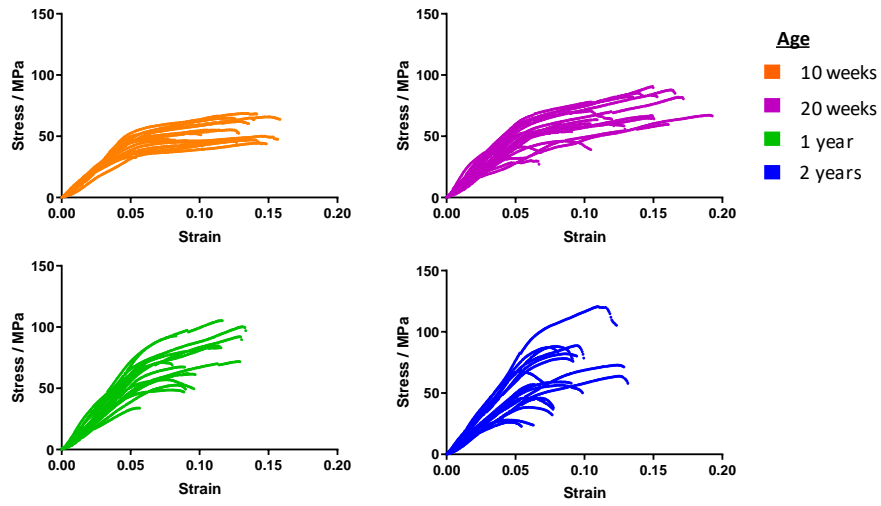


Figure 2 Plots showing representative stress-strain profiles from multiple tendon fibres at four ages. Each age group was sampled from five mice.

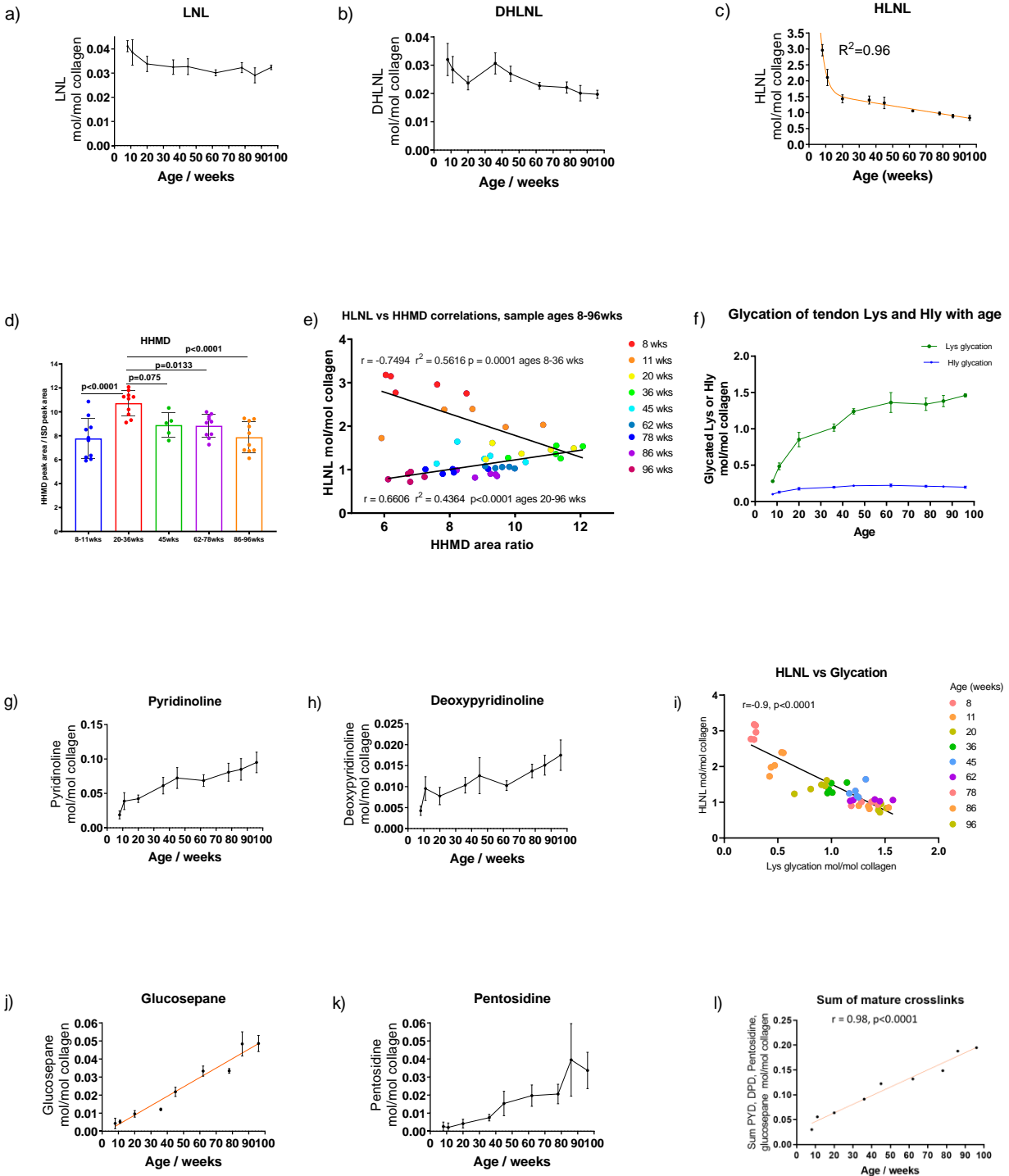


Figure 3a, b, c Graphs showing the levels of the immature crosslinks LNL, DHLNL and HLNL with age in the tendon fibres of C57BL/6 mice ($n=5$ per age group, in duplicate). Statistical analysis: Nonlinear regression fit shown in the HLNL plot (\pm SD). 3d Shows the change in the aldol product HHMD with age. Statistical analysis: ANOVA followed by Tukey's multiple comparisons tests (mean \pm SD, $n=5$ to 10). 3e Shows correlations between HLNL and HHMD with age. Statistical analysis: linear regression. 3f Shows the levels of glycation products with age (mean \pm SD, $n=5$, in duplicate). Lys glycation shown in green, Hly glycation shown in blue. 3g,h,j,k show the development of irreversible crosslinks with age in

the tendon fibres of C57BL/6 mice ($n=5$, in duplicate). statistical analysis of 3j: linear regression fit (\pm SD, $n=5$, in duplicate). 3i Graph showing a correlation between HLNL levels and glycation levels. Statistical analysis: linear regression. 3l The sum of PYD, DPD, Pentosidine and glucosepane mol/mol collagen values plotted against age. Statistical analysis: linear regression.

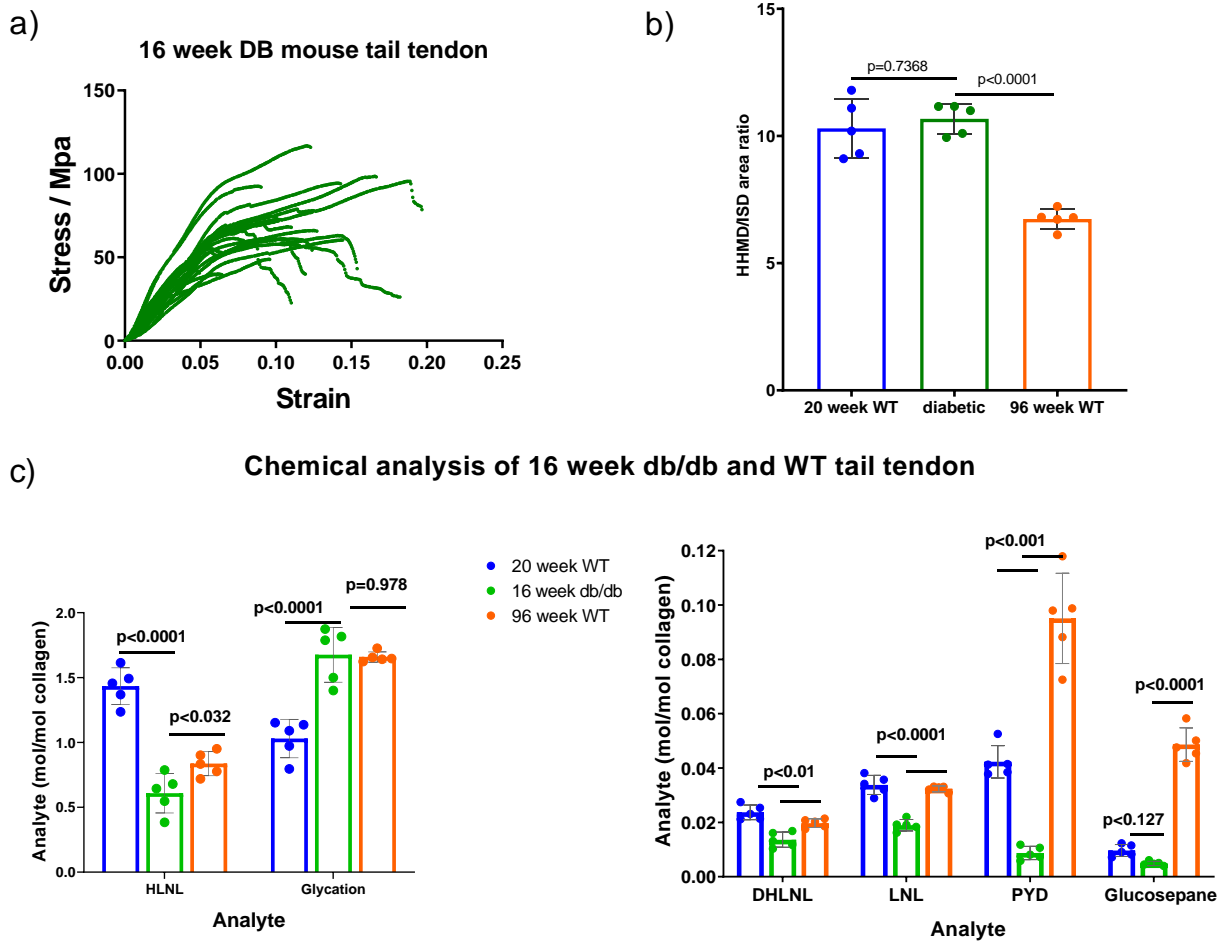


Figure 4a Stress strain plot showing representative tail tendon fibres from five db/db mice. The number of fibres have been limited in this plot so that the shape of the lines can be seen more easily. 4b The HHMD analysis of db/db mouse tail tendon fibres compared with data from WT mice 20 and 96 weeks old (mean \pm SD, $n=5$, in duplicate). Statistical analysis: ANOVA followed by Tukey's multiple comparisons tests. 4c The chemical analysis of db/db mouse tail tendon fibres compared with data from WT mice 20 and 96 weeks old (mean \pm SD, $n=5$, in duplicate). Statistical analysis: ANOVA followed by Tukey's multiple comparisons tests.

Age-related changes in the physical properties, cross-linking, and glycation of collagen from mouse tail tendon

Melanie Stammers, Irina M Ivanova, Izabella S Niewczas, Anne Segonds-Pichon, Matthew Streeter, David A. Spiegel and Jonathan Clark

J. Biol. Chem. published online May 7, 2020

Access the most updated version of this article at doi: [10.1074/jbc.RA119.011031](https://doi.org/10.1074/jbc.RA119.011031)

Alerts:

- [When this article is cited](#)
- [When a correction for this article is posted](#)

[Click here](#) to choose from all of JBC's e-mail alerts